

MEASUREMENT OF THE PROTON ELECTROMAGNETIC FORM FACTORS AT BABAR

V. P. Druzhinin, on behalf of the BABAR Collaboration
*Budker Institute of Nuclear Physics SB RAS, Novosibirsk 630090,
Novosibirsk State University, Novosibirsk 630090, Russia*

Abstract

The process $e^+e^- \rightarrow p\bar{p}$ has been studied in the $p\bar{p}$ mass range from threshold to 6.5 GeV/ c^2 using the initial-state-radiation technique with both detected and undetected photon. The analysis is based on 469 fb $^{-1}$ of integrated luminosity collected with the BABAR detector at the PEP-II collider at e^+e^- center-of-mass energies near 10.6 GeV.

1 Introduction

The energy dependence of the $e^+e^- \rightarrow p\bar{p}$ cross section is given by

$$\sigma_{p\bar{p}}(M_{p\bar{p}}) = \frac{4\pi\alpha^2\beta C}{3M_{p\bar{p}}^2} \left[|G_M(M_{p\bar{p}})|^2 + \frac{\tau}{2}|G_E(M_{p\bar{p}})|^2 \right], \quad (1)$$

where $M_{p\bar{p}}$ is the $p\bar{p}$ invariant mass, $\tau = 4m_p^2/M_{p\bar{p}}^2$, $\beta = \sqrt{1-\tau}$, $C = y/(1-e^{-y})$ is the Coulomb correction factor [1], and $y = \pi\alpha(1+\beta^2)/\beta$. The cross section depends on two form factors, electric G_E and magnetic G_M . From measurement of the cross section we determine the effective form factor

$$F_p(M_{p\bar{p}})^2 = (|G_M(M_{p\bar{p}})|^2 + \frac{\tau}{2}|G_E(M_{p\bar{p}})|^2)/(1 + \frac{\tau}{2}). \quad (2)$$

It should be noted that such a definition was used in all previous measurements made with assumption that G_E is equal to G_M .

The G_M and G_E terms in the differential cross section have different angular dependencies, $1 + \cos^2\theta$ and $\sin^2\theta$, respectively. The ratio of the form factors can be extracted from the analysis of the proton angular distribution. At threshold $G_E = G_M$, and the angular distribution is uniform.

The process $e^+e^- \rightarrow p\bar{p}$ is studied during 40 years [2, 3, 4, 5, 6, 7, 8, 9, 10, 11]. However, all data before recent BABAR [8, 10, 11] and CLEO measurements [7, 9] had an accuracy of 20-30%. The statistics was not sufficient to determine G_E/G_M ratio from angular analysis.

More precise results were obtained in the inverse reaction $p\bar{p} \rightarrow e^+e^-$ [12, 13, 14]. In PS170 experiment [12] at LEAR the proton form factor was measured near threshold. A steep near-threshold mass-dependence was observed. The G_E to G_M ratio was measured with about 30% accuracy and was found to be compatible with unity. Above 3 GeV/ c^2 measurements were performed at Fermilab [13, 14]. The strong decrease of the form factor was observed which agrees with the dependence $M_{p\bar{p}}^{-4}$ predicted by QCD for asymptotic proton form factor. Recently, very precise measurement of the form factor was performed on about 1.4 fb $^{-1}$ data collected by CLEO at 3.77 and 4.17 GeV [9].

2 Initial state radiation technique

The initial-state-radiation (ISR) method is used at BABAR to measure the $e^+e^- \rightarrow p\bar{p}$ cross section. In the ISR reaction $e^+e^- \rightarrow p\bar{p}\gamma$ the photon is emitted by the initial electron or positron. The mass spectrum of the $p\bar{p}$ pair is related to the cross section of the nonradiative process $e^+e^- \rightarrow p\bar{p}$.

The ISR photons are emitted predominantly along beam axis. There are two approaches in ISR measurements: tagged or large-angle (LA) ISR, when the ISR photon is required to be detected, and mainly small-angle (SA) untagged ISR. Only about 10% of the ISR photons can be detected at BABAR calorimeter. The produced $p\bar{p}$ system is boosted against the ISR photon. Due to limited detector acceptance, the $M_{p\bar{p}}$ region below 3 GeV/ c^2 can be studied only with detected photon. Above 3 GeV/ c^2 statistics can be significantly increased with the use of SA ISR.

The advantage of the ISR method over conventional e^+e^- and $p\bar{p}$ experiments is that a wide mass region is studied in a single experiment. The large-angle ISR has additional advantages. The first of them is a low dependence of the detection efficiency on the $p\bar{p}$ invariant mass. Measurement near and above threshold can be done with the same selection criteria. The second is a low dependence of the detection efficiency on hadron angular distributions (in the hadron rest frame). For protons this significantly increases sensitivity for measurements of the G_E/G_M ratio and decreases model uncertainty in the cross section measurement.

Here we present BABAR results based on analysis of 469 fb $^{-1}$ data collected at e^+e^- c.m. energy near 10.6 GeV. Both LA ISR events [10] and SA ISR events [11] have been used for analysis.

The selection of $e^+e^- \rightarrow p\bar{p}\gamma$ candidates requires detection of two charged tracks of opposite charge originating from the interaction region and identified as protons. In LA ISR events a photon with the energy higher than 3 GeV is additionally required. For each LA ISR candidate a kinematic fit with requirement of total energy and momentum conservation is performed. The final selection is based on a condition on χ^2 of the kinematic fit. For SA ISR candidate the selection is based on two parameters: the transverse momentum of the $p\bar{p}$ pair, and the invariant mass of the system recoiling against $p\bar{p}$. Both parameters should be close to zero.

The dominant source of background in the LA case arises from $e^+e^- \rightarrow p\bar{p}\pi^0$ events with an undetected low-energy photon, or with merged photons from the π^0 decay. This background is estimated using a control sample of $e^+e^- \rightarrow p\bar{p}\pi^0$ events. Its level is found to

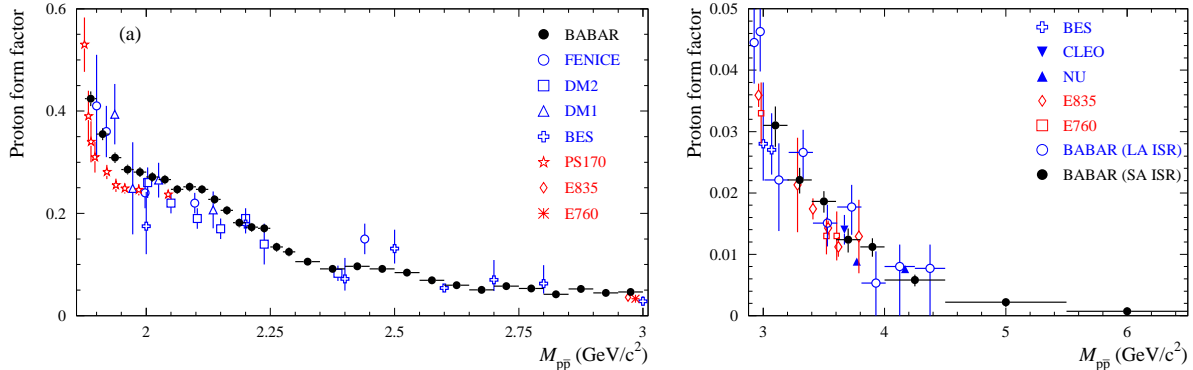


Figure 1: The mass dependence of the effective proton form factor in two different mass region measured by BABAR in comparison with results of previous experiments.

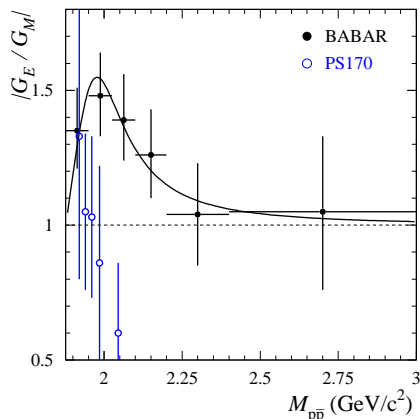


Figure 2: The $|G_E/G_M|$ mass dependence measured by BABAR in comparison with PS170 data.

change from 5% near threshold to 50% at $4 \text{ GeV}/c^2$. All observed $p\bar{p}\gamma$ candidates with the mass greater than $4.5 \text{ GeV}/c^2$ are consistent with $p\bar{p}\pi^0$ background. The contribution of other background processes is estimated to be about 1% of selected data events. The dominant background sources in the SA ISR case are the ISR process $e^+e^- \rightarrow p\bar{p}\pi^0\gamma$ and two-photon $p\bar{p}$ production. The background level is estimated to be about 5% and subtracted.

3 Results

From the measured $p\bar{p}$ mass spectrum we obtain the $e^+e^- \rightarrow p\bar{p}$ cross section and the proton effective form factor. In the mass region under study, the cross section changes by 6 orders of magnitude, from about 1 nb at the $p\bar{p}$ threshold to about 1 fb at $6 \text{ GeV}/c^2$. The measured effective form factor is shown in Fig. 1 in comparison with existing e^+e^- and $p\bar{p}$ data. Our data are in reasonable agreement with previous measurements everywhere except near-threshold region, where the BABAR results are systematically larger than the PS170 data [12].

The measured mass dependence of the ratio $|G_E/G_M|$ is shown in Fig. 2. To measure

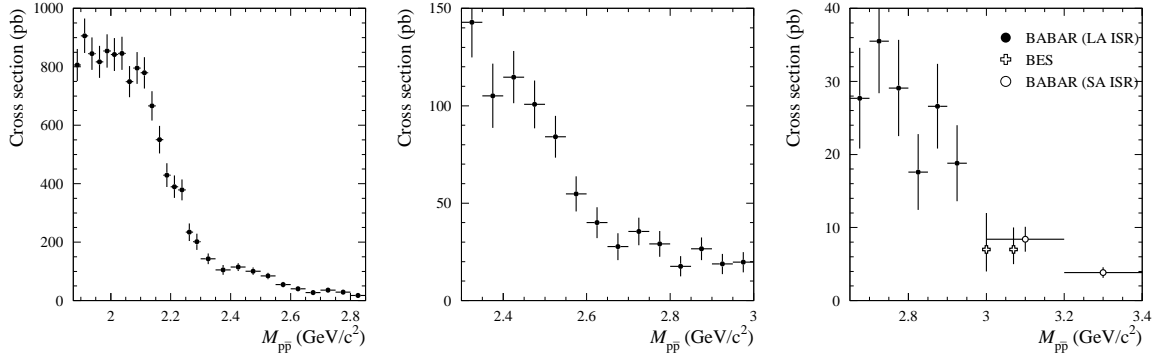


Figure 3: The $e^+e^- \rightarrow p\bar{p}$ cross section in the mass regions near 2.2 (left), 2.5 (middle), and 3 (right) GeV/c^2 .

the ratio the distribution of $\cos\theta_p$ is analyzed, where θ_p is the angle between the proton momentum in the $p\bar{p}$ rest frame and the momentum of the $p\bar{p}$ system in the e^+e^- c.m. frame. The measured ratio is higher than unity at masses below $2.2 \text{ GeV}/c^2$. Our results disagree with the previous PS170 measurement [12].

We have also searched for an asymmetry in the proton angular distribution. An asymmetry is absent in the lowest order (one-photon $p\bar{p}$ production). It arises from higher-order contributions (soft extra ISR and FSR interference, two-photon exchange). The integral asymmetry for events with $p\bar{p}$ mass below $3 \text{ GeV}/c^2$ is found to be consistent with zero:

$$A_{\cos\theta_p} = \frac{\sigma(\cos\theta_p > 0) - \sigma(\cos\theta_p < 0)}{\sigma(\cos\theta_p > 0) + \sigma(\cos\theta_p < 0)} = -0.025 \pm 0.014 \pm 0.003. \quad (3)$$

The measured form factor has a complex mass dependence. The growth of the form factor near threshold as well as the deviation of the ratio $|G_E/G_M|$ from unity may be due to final-state interaction between the proton and antiproton [15]. At higher energies the form factor and cross section display a steplike mass dependence with three steps near 2.2, 2.5, and $3 \text{ GeV}/c^2$. Such a dependence is not described by existing models for the form factors (see, for example, Refs. [16, 17, 18, 19]). The $e^+e^- \rightarrow p\bar{p}$ cross section in the mass regions of the steps is shown in Fig. 3.

Figure 4 depicts the existing form-factor data above $3 \text{ GeV}/c^2$ in log scale. To compensate the main mass dependence of the form factor ($1/m^4$) we also show the scaled (multiplied by $M_{p\bar{p}}^4$) form factor. The dashed curve in Fig. 4 corresponds to a fit of the asymptotic QCD dependence of the proton form factor, $m^4 F_p \sim \alpha_s^2(m)$ [20], to the form factor data. All the data above $3 \text{ GeV}/c^2$ except the two points marked “NU” [9] are well described by this function. Adding the “NU” points changes the fit χ^2/ν from 17/24 to 54/26. Our data shows that the form factor decreases in agreement with the asymptotic QCD prediction. The decrease may be even faster above $4.5 \text{ GeV}/c^2$. The local deviations of the “NU” points from the global fit may be result of the $\psi(3770)$ and $\psi(4160)$ resonance contributions.

The points marked “SLAC 1993” represent data on the space-like magnetic form factor measured in ep scattering [21]. The asymptotic values of the space- and time-like form factors are expected to be the same. In the mass region from 3 to $4.5 \text{ GeV}/c^2$ the time-like

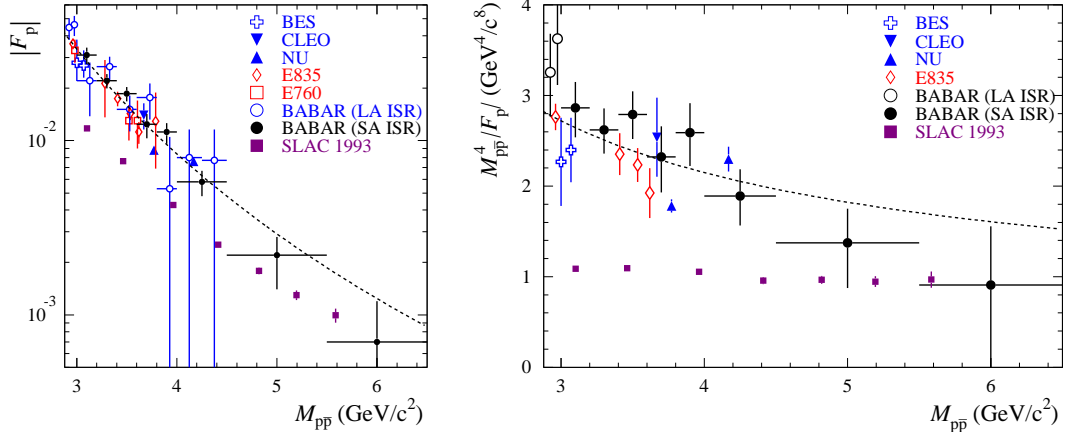


Figure 4: Left plot: the proton effective form factor above $3 \text{ GeV}/c^2$ in log scale. Right plot: the scaled (multiplied by M_{pp}^4) form factor. In the right plot the data points with largest errors were excluded. The points denoted by "SLAC 1993" represent data on the space-like magnetic form factor. The curve is the result of the QCD-motivated fit.

form factor is about two-three times larger than the space-like one. The new BABAR data at high masses give an indication that the difference between the time- and space-like form factors decreases with mass increase.

4 Summary

The $e^+e^- \rightarrow p\bar{p}$ cross section and the proton effective form factor have been measured from threshold up to $6.5 \text{ GeV}/c^2$ using the full BABAR data sample.

The form factor has complex mass dependence. There are a near-threshold steep falloff and a step-like behavior at higher masses. At masses above $3 \text{ GeV}/c^2$ the observed decrease of the form factor agrees with the asymptotic dependence predicted by QCD or is even faster.

The $|G_E/G_M|$ ratio has been measured from threshold to $3 \text{ GeV}/c^2$. A large deviation of this ratio from unity is observed below $2.2 \text{ GeV}/c^2$. The asymmetry in the proton angular distribution has also been measured.

References

- [1] A. B. Arbuzov and T. V. Kopylova, *JHEP* **1204**, 009 (2012).
- [2] M. Castellano *et al.*, *Nuovo Cim. A* **14**, 1 (1973).
- [3] B. Delcourt *et al.* (DM1 Collaboration), *Phys. Lett. B* **86**, 395 (1979).
- [4] D. Bisello *et al.* (DM2 Collaboration), *Nucl. Phys. B* **224**, 379 (1983); *Z. Phys. C* **48**, 23 (1990).

- [5] A. Antonelli *et al.* (FENICE Collaboration), Nucl. Phys. B **517**, 3 (1998).
- [6] M. Ablikim *et al.* (BES Collaboration), Phys. Lett. B **630**, 14 (2005).
- [7] T. K. Pedlar *et al.* (CLEO Collaboration), Phys. Rev. Lett. **95**, 261803 (2005).
- [8] B. Aubert *et al.* (BABAR Collaboration), Phys. Rev. D **73**, 012005 (2006).
- [9] K. K. Seth *et al.*, Phys. Rev. Lett. **110**, 022002 (2013).
- [10] J. P. Lees *et al.* (BABAR Collaboration), Phys. Rev. D **87**, 092005 (2013).
- [11] J. P. Lees *et al.* (BABAR Collaboration), Phys. Rev. D **88**, 072009 (2013).
- [12] PS170 Collab. (G. Bardin *et al.*), Nucl. Phys. B **411**, 3 (1994).
- [13] T. A. Armstrong *et al.* (E760 Collaboration), Phys. Rev. Lett. **70**, 1212 (1993).
- [14] M. Ambrogiani *et al.* (E835 Collaboration), Phys. Rev. D **60**, 032002 (1999); M. Andreotti *et al.*, Phys. Lett. B **559**, 20 (2003).
- [15] V. F. Dmitriev, A. I. Milstein and S. G. Salnikov, arXiv:1307.0936 [hep-ph].
- [16] M. A. Belushkin, H.-W. Hammer and Ulf-G. Meissner, Phys. Rev. C **75**, 035202 (2007).
- [17] J. P. B. C. de Melo *et al.*, Phys. Lett. B **671**, 153 (2009).
- [18] S. Furuichi, H. Ishikawa and K. Watanabe, Phys. Rev. C **81**, 045209 (2010).
- [19] E. L. Lomon and S. Pacetti, Phys. Rev. D **85**, 113004 (2012); erratum-ibid. D **86**, 039901 (2012).
- [20] V. L. Chernyak and A. R. Zhitnitsky, JETP Lett. **25**, 510 (1977); G. P. Lepage and S. J. Brodsky, Phys. Rev. Lett. **43**, 545 (1979).
- [21] A. F. Sill *et al.*, Phys. Rev. D **48**, 29 (1993).